

Interactive comment on “Time Series Analysis of Ground-Based Microwave Measurements at K- and V-Bands to Detect Temporal Changes in Water Vapor and Temperature Profiles” by Sibananda Panda et al.

Sibananda Panda et al.

swaroop.sahoo769@gmail.com

Received and published: 24 October 2016

The authors would like to thank the reviewer for the comments which have significantly improved the quality of the paper.

Comment: 1) To improve the dissemination of the manuscript, please add a paragraph describing the physical phenomenon at the basis of the sensing.

Response: The authors have added the following paragraph to the paper in Section 3.1. Remote sensing of water vapor and temperature is based on the measurement of microwave radiation emitted by water vapor and oxygen molecules. The emission

and absorption of microwave radiation due to water vapor and oxygen in each tropospheric layer change the microwave radiation that reaches the ground. This variation in radiation is due to the concentration of water vapor in the atmosphere and the temperature at various altitudes. Therefore, these microwave radiation reaching the ground are source of information about the humidity distribution and temperature variation in the atmosphere at different heights. Measurement of this radiation at the weak water humidity absorption line (centred at 22.235 GHz) is used for the sensing of water vapor profile variation. This is based on humidity absorption line broadening. This broadening is due to motion of the water molecules and their collisions with other water molecules and is known as pressure broadening. Thus change in pressure has a significant impact on the width of the absorption lines as well as the absorption values. So, a decrease in the atmospheric pressure reduces the line width and increases the water vapor absorption line strength which is most prominent at 22.235 GHz (the center of the absorption line). Therefore, closer the proximity of the measurement frequency to the weak water vapor resonance frequency higher the sensitivity to water vapor at high altitudes. As the pressure increases the absorption line widens resulting in reduced sensitivity to water vapor at high altitudes. However, frequencies farther away from the center frequency are more sensitive to water vapor changes close to ground level. This is again proven by the weighting functions at various frequencies. Weighting functions closest to the water vapor resonance frequencies are almost twice more sensitive to water vapor at 8 km than near ground level. While frequencies further way from the resonance peak are most sensitive to changes close to ground level. Therefore, a combination of various frequency measurements is able to detect the profile information about water vapor. Similarly, microwave radiation from oxygen at the 60 GHz absorption complex can be used for retrieving temperature profile information because atmospheric absorption in the 50-75 GHz range is primarily due to oxygen molecules. The absorption due to oxygen molecule is due to magnetic moment 33 spin-rotational lines between 51.5-67.9 GHz. These spin-rotational lines blend together at lower altitude due to the pressure broadening of the lines. This blended absorption lines has a

shape similar to an absorption band centered at 60 GHz. However, the absorption line intensity is not the simple addition of isolated line intensities but the "overlap interference" which gives rise to a very complex absorption band called the oxygen complex. As a result the opacity at the 60 GHz is significantly higher than that at 50 GHz, so the radiometer just observes the radiation emitted close to the ground surface. To sample the whole troposphere measurements need to be performed at a number of frequencies away from the center frequency. Since, oxygen is the most well mixed gas in the atmosphere and its proportion in the atmosphere is almost constant and altitude independent from ground level to 80 km, the microwave radiation at the oxygen absorption lines contains atmospheric temperature profile information.

Comment: 2) For the Bayesian Optimal Estimation section: 2.1 If the equation (1) is the updating iterative minimization step of the cost function in eq. (2), it is necessary to define first the cost function and after to provide the minimization step. In other words, please eq.(1) becomes eq.(2) and eq.(2) becomes eq. (1).

Response: Eq. (2) has become Eq. (3). The authors agree that the iterative minimization step of the cost function in Eq. (3) comes after the definition of the cost function. However, the authors would like to stress that the first step is to determine the updated water vapor and temperature profiles using the iterative process Eq. (1) which are then validated using the cost function Eq. (3) as well as the convergence criterion Eq. (4). Therefore, the sequence of the equations is maintained as it is.

Comment: 2.2 How do you choose the value of m in eq. (3) to define the convergence criterion?

Response: Eq. (3) has become Eq. (4). The following has been added to Section 3.2.1 line 12 of Page 7. "Eq. (4) determines the termination of the iterative process. The iteration stops when Eq. (4) reaches a value q which is very small in comparison to m . Therefore, the value of q is chosen to be 0.05 and 0.07 for water vapor and temperature profile retrieval, respectively, which is 1/100 times the number of measurements used."

[Printer-friendly version](#)[Discussion paper](#)

Comment: 2.3 Please, comment more in detail about the effect of parameter γ on the local minima problem.

Response: As per the reviewer suggestion the calculation of γ has been discussed in detail and has been illustrated with Figure 4. The following has been added Section 3.2.1 Page 6 line 26. γ is the LM factor and the value of γ is updated at each iteration based on value of $J(x)$ from Eq. (3). Various initial values of γ in the range of $\gamma=1$ and $\gamma=\infty$ have been considered for starting of the iteration. For $\gamma = 1$, the iteration might move towards a local minima while in case of $\gamma=\infty$ the iteration immediately moves towards the global minima which gives a solution which does not converge. Therefore, the initial value of γ is assumed to be one. It was observed that the algorithm did not converge with a valid output for this initial value of gamma so the initial value of gamma is increased at regular intervals to check the convergence. It was found empirically, that gamma with an initial value of 5000 converges the algorithm for all cases. As part of the iteration if the value of $J(x)$ increases, then the iteration is discarded and the value of γ is increased 10 fold and the iteration is repeated. This is done so as to discard any invalid output which could be close to one of the local minima. If value of $J(x)$ decreases, then the iteration is valid and the value of γ is reduced by a factor of 2 for the next iteration even if the convergence criteria is not satisfied (Hewison, 2007). This process is followed until the convergence criterion is validated by the output profile. This process is illustrated in Figure 4. It can be observed that as the cost function decreases, the gamma value decreases and vice versa. At local minima of the cost function the gamma value also reduces.

Comment: 3) The section about the Neural Network (NN) estimation should be enlarged. What is the number of the unknowns searched for in the NN estimation? How long was the time to train the network?

Response: As per the suggestion of the reviewer the following detail has been added to the neural network retrieval technique in Section 3.3. "Estimation of water vapor and temperature profiles from microwave radiometer brightness temperatures is done us-

[Printer-friendly version](#)[Discussion paper](#)

ing a proprietary neural network method (NN) developed by Radiometrics Corporation (Solheim, et al., 1998). NN zenith estimation of temperature, water vapor density, relative humidity, and liquid water content profiles are performed simultaneously from the radiometer measurements plus the infrared (IR) channel. The retrieved profiles are estimated at 58 height levels, with 50 meter steps from the surface up to 500 m, then 100 m steps to 2 km, and 250 m steps from 2 to 10 km. However, it has to be noted that above approximately 7 km, the atmospheric water vapor density and temperature approach the climatological mean values. As part of the retrieval process the NN is trained using a back-propagation algorithm and radiosonde data which has been collected over a period of time i.e., usually 4 to 5 years using. The radiosonde data that is used for training the network is taken from one or more sites with the same climatological conditions as the observation site. The radiosonde profiles are used for simulating the brightness temperature using absorption models and radiative transfer equations. The NN estimation uses a standard feed-forward network (Radiometrics Corporation, 2008) to retrieve the temperature, humidity and liquid water profile that is most consistent with the atmospheric conditions and radiometric measurements. However, in this case sufficient radiosonde profiles were not available for Mahabubnagar, so a slightly different approach was used in this study for neural network estimation of profiles. Radiosonde profiles were still used as training dataset but these were taken from areas which had similar weather conditions and same altitude and latitude (but different longitude) as Mahabubnagar, Hyderabad. However, two sites at the same altitude and longitude may have significantly different weather depending on the general conformation of the mountains in the area, the marine currents as well as the advection processes. This could lead to biases in the training of the radiometer algorithm which in turn would increase the error of the retrieved profile.”

Comment: 4) By looking to Figure 8, please comment the fact (maybe, by providing a “physical justification”) that the RMS error for NN estimation, has a decreasing behaviour with kilometres for the water content profile whereas increases with the distance for the temperature profile.

Response: Figure 8 has become Figure 11. The following discussion has been added as the last paragraph of Section 4.3 on page 12 line 1. “It has to be observed that that the RMS error for NN estimated water vapour density profile has a decreasing behaviour with altitude whereas the temperature profile RMS error increases with the height for the temperature profile. This is because NN algorithm used to retrieve the water vapor and temperature profiles has been trained using a data set which has been taken from areas which had similar weather conditions as the radiometer observation site. However, two sites at the same altitude and longitude may have significantly different weather depending on the general conformation of the mountains in the area, the marine currents as well as the advection processes. This could lead to biases in the training of the radiometer algorithm which in turn would increase the error of the retrieved profile. This is what is causing the retrieval errors for both the water vapor and temperature profiles at the lower altitudes. However, at high altitudes the range of water vapor density values which are possible are limited and close to zero as they cannot be less than zero, (obviously the climatological mean) due to which the error levels reduce at high altitudes as shown in Figure 11(a). This is not the case for temperature profiles which can have really low values at high altitudes based on training data. Therefore, the temperature profiles have a high level of bias, hence the increase in error as the altitude increases.”

Please also note the supplement to this comment:

<http://www.geosci-instrum-method-data-syst-discuss.net/gi-2016-16/gi-2016-16-AC6-supplement.pdf>

Interactive comment on Geosci. Instrum. Method. Data Syst. Discuss., doi:10.5194/gi-2016-16, 2016.

[Printer-friendly version](#)

[Discussion paper](#)



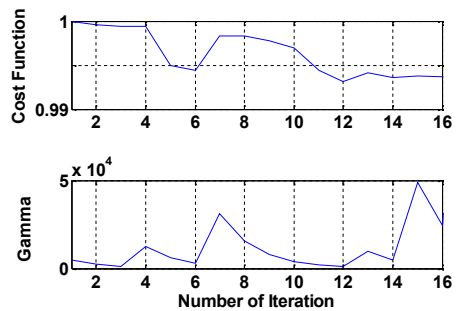


Figure 4. The value of cost function and gamma with respect to number of iterations are shown in the top and bottom figure, respectively.

Fig. 1. Figure 4